Phase Behavior and Bilayer Properties of Fatty Acids: Hydrated 1:1 Acid–Soaps†

David P. Cistola,* David Atkinson,‡ James A. Hamilton, and Donald M. Small

Departments of Medicine and Biochemistry, Biophysics Institute, Housman Medical Research Center, Boston University School of Medicine, Boston, Massachusetts 02118

Received September 25, 1985; Revised Manuscript Received January 24, 1986

ABSTRACT: The physical properties in water of a series of 1:1 acid–soap compounds formed from fatty acids and potassium soaps with saturated (10–18 carbons) and ω-9 monounsaturated (18 carbons) hydrocarbon chains have been studied by using differential scanning calorimetry (DSC), X-ray diffraction, and direct and polarized light microscopy. DSC showed three phase transitions corresponding to the melting of crystalline water, the melting of crystalline lipid hydrocarbon chains, and the decomposition of the 1:1 acid–soap compound into its parent fatty acid and soap. Low- and wide-angle X-ray diffraction patterns revealed spacings that corresponded (with increasing hydration) to acid–soap crystals, hexagonal type II liquid crystals, and lamellar liquid crystals. The lamellar phase swelled from bilayer repeat distances of 68 (at 45% H_2O) to 303 Å (at 90% H_2O). Direct and polarized light micrographs demonstrated the formation of myelin figures as well as birefringent optical textures corresponding to hexagonal and lamellar mesophases. Assuming that 1:1 potassium hydrogen dioleate and water were two components, we constructed a temperature–composition phase diagram. Interpretation of the data using the Gibbs phase rule showed that, at >30% water, hydrocarbon chain melting was accompanied by decomposition of the 1:1 acid–soap compound and the system changed from a two-component to a three-component system. Comparison of hydrated 1:1 fatty acid/soap systems with hydrated soap systems suggests that the reduced degree of charge repulsion between polar groups causes half-ionized fatty acids in excess water to form bilayers rather than micelles. The 1:1 fatty acid/soap system provides insights into the physical states formed by free fatty acids during transport and metabolism in vivo since, at pH 7.4, fatty acids in water and in phospholipid bilayers are near half-ionization.

The physical properties of "fatty acids"[1] in water are largely influenced by the ionization state of the carboxyl group (Small, 1968). "Fatty acid"/water systems have been studied extensively at the extremes of ionization, and their physical properties are well-known [for recent reviews, see Taylor and Princen (1979) and Small (1986)]. For example, fully ionized fatty acids (soaps) form micelles, liquid crystals, or crystals in water whereas fully un-ionized fatty acids form oil droplets or crystals. However, the physical states formed at intermediate degrees of ionization are not well-known, and most of the work on these systems was done many years ago, often on impure systems.

As early as 1823, sediments were observed in partially hydrolyzed soap solutions (Chevreul, 1823). These sediments were called acid–soaps because they had a composition intermediate between those of fully un-ionized fatty acids and ionized soaps. Later, the systematic phase rule studies of McBain and co-workers demonstrated that anhydrous acid–soaps are unique compounds that contain fixed stoichiometries of 1:1, 1:2, or 2:1 fatty acid to soap (McBain & Field, 1933a,b; McBain & Stewart, 1927, 1933). The powder X-ray diffraction studies of Piper demonstrated that crystalline 1:1 acid–soap compounds with saturated acyl chains exhibited long spacings distinct from those of crystalline fatty acids or soaps (Piper, 1929).

In spite of the early interest in anhydrous acid–soaps, the physical properties of long-chain acid–soaps in water have received very little attention. Light microscopic observations demonstrated that acid–soaps in water above their melting temperature form myelin figures analogous to those formed by phospholipids in water (Ekwall, 1937). This phenomenon was later observed with phase contrast and freeze–fracture electron microscopy for partially ionized unsaturated (Gebicki & Hicks, 1973) and saturated (Hargreaves & Deamer, 1978) fatty acids in water.

We present the first systematic X-ray diffraction study of 1:1 acid–soaps in water. Combining X-ray diffraction with differential scanning calorimetry and direct and polarized light microscopy, we show that saturated (10–18 carbons) and the ω-9 monounsaturated (18 carbons) 1:1 fatty acid/potassium soap systems in water spontaneously form crystalline and liquid-crystalline aggregates, including inverted hexagonal and bilayer structures. A temperature–composition phase diagram for 1:1 oleic acid/potassium oleate in water is presented. These findings have application to the study of bilayer and other liquid-crystalline structures and yield information about the forces that stabilize liquid-crystalline mesophases. Also, 1:1 fatty acid/soap systems provide insights into the physical states

† This work was supported by U.S. Public Health Service Grants HL-26335 and HL-07291 and was submitted in partial fulfillment of the requirements for the degree of Doctor of Philosophy at Boston University, 1985. Preliminary accounts of this work were presented at the Annual Meetings of the American Oil Chemist's Society (Honored Student Presentation), Chicago, IL, May 1983, and the Biophysical Society, Feb 1985, and have been published in abstract form (Cistola et al., 1983, 1985).

‡ Established Investigator of the American Heart Association.

[1] In this paper, "fatty acids" (when enclosed by quotation marks) refers to the general class of compounds without specification of the ionization state of the carboxyl group. Thus, "fatty acids" could refer to fully un-ionized fatty acids, fully ionized fatty acids (soaps), mixtures of ionized and un-ionized species, and/or 1:1 acid–soap compounds. The term fatty acids (when used *without* quotation marks or qualifying phrases) specifically refers to fully un-ionized (protonated) fatty acids.

0006-2960/86/0425-2804$01.50/0 © 1986 American Chemical Society

formed by nonesterified (free) "fatty acids" in vivo since, at pH 7.4, long-chain "fatty acids" in water (above their monomer solubility limit) and in phospholipid bilayers are near half-ionization (Barratt & Laggner, 1974; Kantor & Prestegard, 1978; Ptak et al., 1980; Cistola, 1985; Hamilton & Cistola, 1986).

Materials and Methods

Preparation and Analysis of Acid–Soap Crystals. Potassium hydrogen dioleate, decanoate, laurate, myristate, palmitate, and stearate (all 1:1 acid–soaps) were crystallized from ethanol as described previously (Goddard et al., 1968) by using fatty acids and potassium soaps (both >99%, Nu Chek Prep, Elysian, MN) as starting materials. These starting materials were used without further purification or analysis. The resulting 1:1 acid–soap crystals were analyzed as follows: (i) the 1:1 stoichiometry of fatty acid to soap was confirmed by titration in ethanol as described previously (Goddard et al., 1968), (ii) the presence of acid–soap melting transitions and the absence of fatty acid melting transitions were confirmed by DSC[2] and microscopy, and (iii) the presence of long spacings corresponding to crystalline 1:1 acid–soap and the absence of long spacings corresponding to either crystalline fatty acid or potassium soap were confirmed by powder X-ray diffraction; this distinction is possible because the long spacings of 1:1 acid–soap crystals are different from those for either fatty acid or soap crystals (Piper, 1929).

Preparation and Equilibration of Hydrated Samples. Hydrated samples were prepared by weighing 1:1 acid–soap crystals and doubly distilled, deionized water into glass tubes containing a narrow constriction. The tubes were flame-sealed under nitrogen. Equilibration was promoted by heating samples to a temperature above the chain-melting transition for hydrated samples and repeatedly centrifuging the samples through the narrow constriction. All hydrated samples were equilibrated for a minimum of 1 week at temperatures 10–20 °C above their corresponding chain-melting transitions. After equilibration, the tubes were broken open, and aliquots were transferred (within 15 min) to stainless steel DSC pans for calorimetric analysis, 1-mm quartz capillary tubes (Charles Supper Co., Natick, MA) for X-ray analysis, and glass microscope slides with cover slips for microscopic analysis. Although significant water evaporation during sample transfer (15 min) was unlikely, this possibility was further assessed by measurements of ΔH (ice melting) as a function of weight percent water (see Results and Figure 1C). X-ray capillaries were flame sealed under N_2, and the ends were reinforced with a small amount of quick drying (5-min) epoxy. Glass slides were permanently sealed by applying epoxy around the edges of the cover slip. No yellowing or changes in gross sample appearance or water content were noted over the period of data collection (>1 year).

Differential Scanning Calorimetry. Heating and cooling scans (5 °C/min) were performed on a DSC-2 calorimeter (Perkin-Elmer, Norwalk, CT) calibrated with gallium. Transition temperatures were determined by extrapolating the slope of the onset of the transition to the base line. Base lines in the region of the transition were aproximated by extrapolating the pretransition base line to the posttransition base line. Enthalpy measurements were determined from the area under the transition peak by comparison with areas for a known standard (gallium).

X-ray Diffraction. Capillaries containing samples were placed in a sample holder kept at constant temperature by a circulating antifreeze/water bath. Nickel-filtered Cu Kα X-radiation (λ = 1.5418 Å) from a microfocus X-ray generator (Jarrell-Ash, Waltham, MA) was focused by a single nickel-coated mirror and further collimated by a Luzzati-Baro camera with slit optics. Low- and wide-angle diffraction patterns were recorded with a position-sensitive detector (Tennelec PSD-1100, Oak Ridge, TN) and a computer-based analysis system (Tracor Northern TN-1710, Middleton, WI).

Direct and Polarized Light Microscopy. In addition to the equilibrated microscopy samples prepared as above, additional samples were prepared by placing a small amount of finely ground crystalline acid–soap between a glass slide and coverslip and adding several drops of water to the edge of the coverslip (Small et al., 1966). All samples were examined by direct and polarized light with a polarizing microscope (Leitz Dialux, Wetzlar, West Germany) fitted with a heating/cooling stage (Model 80, Leitz) and a thermocouple/digital thermometer (Doric Model 450, San Diego, CA). Changes in optical texture were observed during heating and cooling scans (1 °C/min) in the temperature range 0–70 °C.

Results

Analysis of Composition and Properties of Anhydrous Acid–Soap Crystals. The fatty acid content of the 1:1 potassium hydrogen dioleate crystals determined by titration was 45.6 ± 1.0% (w/w; mean of three determinations ± standard deviation); the expected value for a 1:1 compound is 46.8% (w/w). DSC and microscopic analysis of crystals heated from 20 to 70 °C showed one sharp melting transition at 47 °C, as expected for 1:1 potassium hydrogen dioleate (McBain & Stewart, 1933). Microscopic and X-ray analysis above 47 °C demonstrated that the sample consisted of crystals of potassium oleate (first-order *d* spacing, 44 Å) in an isotropic liquid; thus, the anhydrous 1:1 acid–soap compound decomposed at 47 °C, as expected (McBain & Stewart, 1933). Powder X-ray diffraction patterns at 25 °C yielded 7 orders of reflection indexing into a one-dimensional lamellar geometry. Table I illustrates that the observed first-order reflection for anhydrous crystalline 1:1 potassium hydrogen dioleate (47.1 ± 0.5 Å) differed significantly from that for potassium oleate (44.0 ± 0.5 Å) or oleic acid (40.9 ± 0.3 Å). These differences were also seen with saturated 1:1 potassium acid–soaps and their corresponding potassium-saturated soaps and fatty acids [Table I; see also Piper (1929)]. For the 1:1 acid–soaps, a plot of first-order *d* spacing vs. hydrocarbon chain length yielded a slope of 1.3 Å per CH_2 group, indicating that the axis of the lipid molecules is essentially perpendicular to the bilayer plane; this is consistent with Piper's (1929) original observations. Thus, analysis of the composition and properties of the anhydrous compounds obtained from crystallization in ethanol demonstrated that the stoichiometry was 1:1 fatty acid to soap, the compounds were free from contamination by fatty acid or potassium soap, and the anhydrous compounds had the same physical properties and/or powder diffraction patterns as those previously documented for 1:1 acid–soaps (McBain & Stewart, 1927, 1933; Piper, 1929). This confirms that compounds utilized in this study were 1:1 acid–soaps.

Differential Scanning Calorimetry. Figure 1 shows selected DSC tracings (Figure 1A), heating transition temperatures (Figure 1B), and enthalpies (Figure 1C) as a function of water concentration for 1:1 potassium hydrogen dioleate. Samples were cycled several times between −33 and 57 °C (10% H_2O sample), −28 and 47 °C (20% H_2O sample), or −28 and 27 °C (all other samples). All transitions were reversible upon

[2] Abbreviations: DSC, differential scanning calorimetry; *F*, number of degrees of freedom; *C*, number of components; *P*, number of phases; *d*, first-order X-ray long spacing (Bragg spacing).

Table I

chain type	d (Å), FA Cr[a]	d (Å), K soap Cr[b]	d (Å), 1:1 acid-soap Cr[c]	hydrated acid-soap (80% H_2O) d (Å)[d]	phase[e]	T_m (°C)[f]
decanoate	22.8	27.4	30.1	111	lam	22
laurate	27.1	29.9	35.3	115	lam	34
myristate	33.8	36.5	39.6	133	lam	43
palmitate	35.7	37.7	45.2	96[g]	lam[g]	51[g]
	41.3					
	43.7					
stearate	39.8	42.4	51.2	148	lam	61
	43.7					
	~50					
oleate	40.9	44.0	47.1	173	lam	11

[a] First-order d spacings for anhydrous crystalline fatty acids at 25 °C. Multiple values for palmitate and stearate represent polymorphic forms. [b] First-order d spacings for anhydrous crystalline potassium soaps at 25 °C. [c] First-order d spacings for anhydrous crystalline 1:1 potassium acid-soaps at 25 °C. [d] First-order d spacings for *hydrated* 1:1 potassium acid-soaps at 80% water and at a temperature *above* the melting transition noted in the rightmost column. The specific sample temperatures were 25 (decanoate), 45 (laurate), 56 (myristate), 64 (palmitate), 64 (stearate), and 20 °C (oleate). [e] Type of liquid-crystalline phase as observed by X-ray diffraction for hydrated 1:1 potassium acid-soaps at 80% water at the temperatures noted in footnote *f*. Abbreviation: lam, lamellar liquid-crystalline phase. [f] Chain-melting transition of hydrated 1:1 potassium acid-soap at 80% water as determined by DSC. [g] Values for samples containing 70% water.

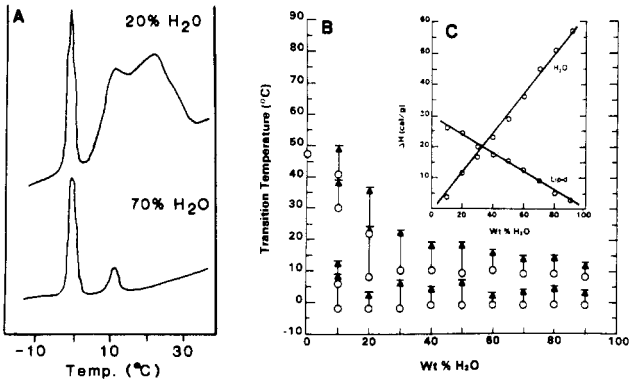

FIGURE 1: Selected DSC tracings (A), transition temperatures (B), and enthalpies (C) upon heating as a function of water concentration for hydrated 1:1 potassium hydrogen dioleate. For plot B, open circles represent the onset, and the tips of the arrow the completion, of the transition. The heating rate was 5 °C/min. For plot C, enthalpies are in units of calories per gram of total sample. The enthalpy line labeled "H_2O" corresponds to the first heating transition (at −1 °C), and the enthalpy line labeled "lipid" corresponds to the summation of all other heating transitions for a given sample. For samples with >20% H_2O, there is only one lipid transition. For samples containing ≤20% H_2O, the values of onset and completion temperatures contain a relatively large estimated uncertainty (±4 °C) because of broad, partially overlapping lipid transitions.

recycling but had an undercooling effect ranging from 2 (10% H_2O sample) to 14 °C (90% H_2O sample) for lipid cooling transitions and from 19 (10% H_2O sample) to 13 °C (90% H_2O sample) for water cooling transitions.

Plots of ΔH for the water melting transition and for the sum of all lipid melting transitions were linear and extrapolated to zero enthalpy at 0% and 100% water, respectively (Figure 1C). These results suggested that significant water evaporation did not occur during sample preparation and transfer.

Chain-melting transitions obtained by DSC for saturated 1:1 acid-soaps (in 80% water) are given in Table I.

X-ray Diffraction. Figure 2 shows selected low-angle X-ray diffraction patterns for 1:1 potassium hydrogen dioleate in water at 20 °C. At 40% H_2O, 3 orders of reflections were observed. The long spacings occurred in a ratio of $1:(1/\sqrt{3}):(1/\sqrt{4})$ and indexed into a two-dimensional hexagonal lattice (Luzzati, 1968). At 50% and 60% H_2O, an additional set of reflections were seen; these occurred in a ratio of $1:{}^1/_2:{}^1/_3$ and indexed into a one-dimensional lamellar lattice. At 80% water, four lamellar and no hexagonal reflections were observed, and at 90% water, two lamellar reflections and a broad scattering fringe were observed.

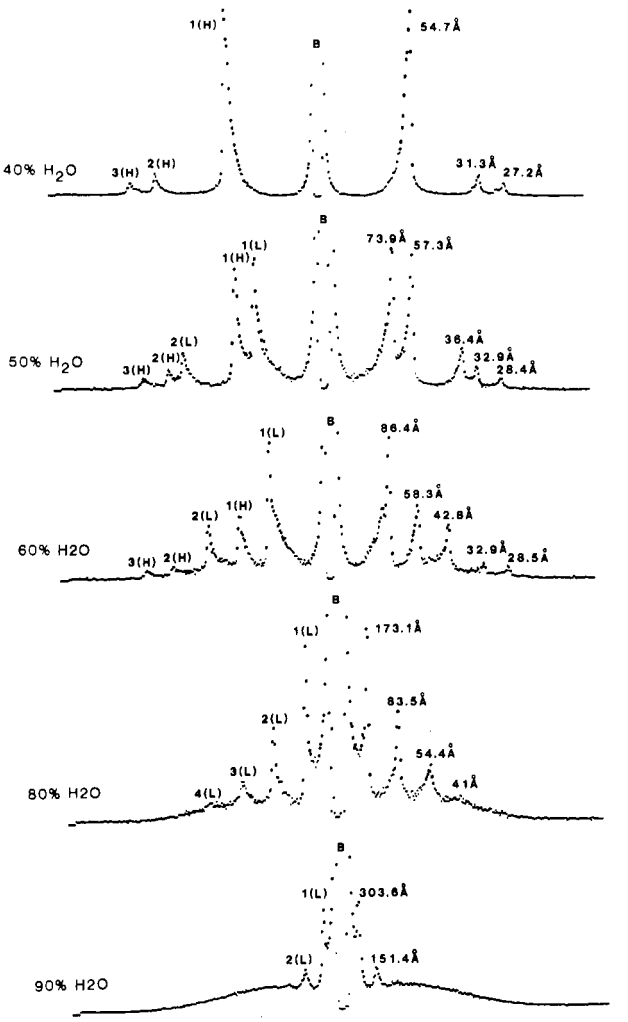

FIGURE 2: Low-angle X-ray diffraction patterns for 1:1 potassium hydrogen dioleate at different water concentrations at 20 °C. The sample of detector distance was 400 mm. The center doublets labeled "B" represent residual intensity from the central X-ray beam which has been partially blocked by a backstop. All other peaks represent X-rays diffracted by the sample. The peaks to the left of the central beam are a mirror image of, and correspond to, those on the right. On the left, peaks are labeled according to their diffraction order (Bragg's law) and phase, and on the right, according to their Bragg spacing in angstroms. Abbreviations: H, hexagonal; L, lamellar.

Figure 3 shows a plot of low-angle diffraction data for 1:1 potassium hydrogen dioleate as a function of water concentration at 20 °C. The type of phases observed depended upon

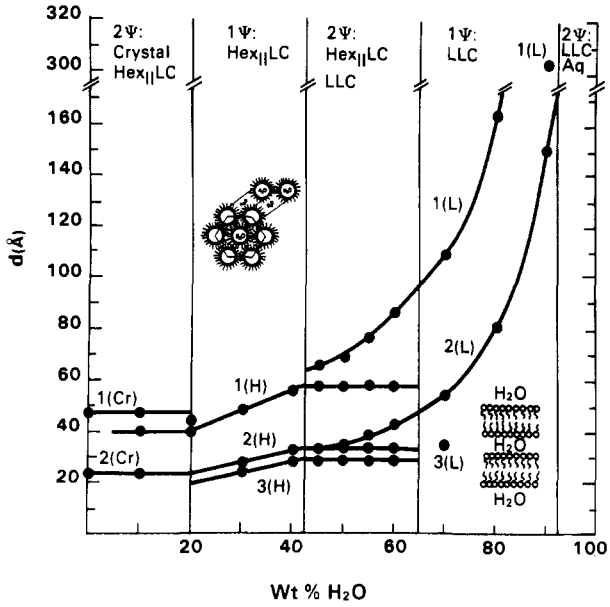

FIGURE 3: Low-angle X-ray diffraction *d* spacings as a function of water concentration for hydrated 1:1 potassium hydrogen dioleate at 20 °C. Abbreviations: Hex$_{II}$ LC, hexagonal type II liquid-crystalline phase; LLC, lamellar liquid-crystalline phase; Ψ, phase(s); Aq, aqueous phase; wt, weight; 1, 2 and 3, first-, second-, and third-order reflections, respectively; Cr, H, and L, crystalline, hexagonal, and lamellar reflections, respectively.

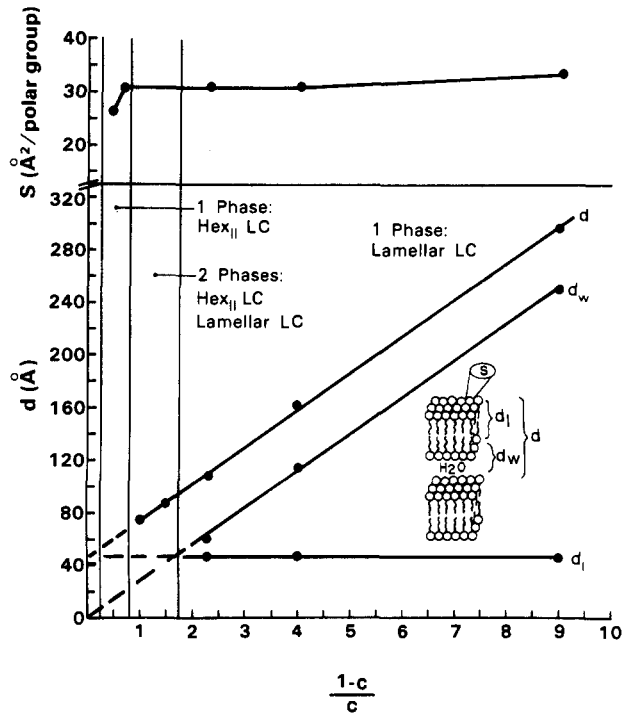

FIGURE 4: Low-angle X-ray diffraction first-order long spacings (*d*), surface areas per polar group (*S*), lipid layer thickness in the presence of water (d_L), and water thickness (d_W) as a function of $(1 - c)/c$ (where *c* represents weight fraction of lipid) for hydrated 1:1 potassium hydrogen dioleate at 20 °C. *S* and d_W were calculated by using the equations of Luzzati (1968); see Results. For all calculations, d_L was assumed to be 47 Å; this value was obtained by extrapolation of *d* to zero water content or $(1 - c)/c = 0$ (see Discussion). All points in this figure pertain to the lamellar phase except for *S* values at $(1 - c)/c < 1$, which correspond to the hexagonal phase.

the water content and, with increasing water content, were crystalline (Cr), hexagonal (H), and lamellar (L). The crystalline reflections were identical with those for anhydrous crystalline 1:1 potassium hydrogen dioleate (Table I). Wide-angle diffraction data (not shown) for samples with >20% water at 20 °C revealed only a broad fringe centered at 4.5 Å; this indicated that the hydrocarbon chains were liquid (Müller, 1932; Luzzati, 1968). Thus, the hexagonal and lamellar arrays were liquid crystalline. Surface areas per polar group were calculated by using the equations given in Luzzati (1968) and by assuming the density of the lipid was roughly that of liquid long-chain fatty acids (0.82 g/cm^3; Small, 1986) and was constant with increasing water concentration. The calculated surface areas for the hexagonal phase increased from 27 (30% water) to 31 Å^2 (40% water) per polar group. Surface areas for the lamellar phase remained roughly constant at 33 Å^2 per polar group (Figure 4).

With increasing water content, the lamellar phase swelled to give first-order *d* spacings >300 Å at 90% water (Figure 3). Even at these large interbilayer spacings, two sharp first- and second-order lamellar reflections were seen (Figure 2). Above 90% water, order was lost and only a very broad scattering fringe was seen. For the lamellar phase, a plot of first-order *d* spacings (20 °C) vs. $(1 - c)/c$ (Figure 4) was linear and extrapolated to 46 Å at $(1 - c)/c = 0$; this value is identical with the first-order reflection for anhydrous 1:1 potassium hydrogen dioleate crystals.

A plot of *d* spacings at 40 °C as a function of weight percent H_2O (data not shown) was similar in shape to the plot at 20 °C (Figure 3) except in the low-water region, where no crystalline phase was found.

Low-angle diffraction patterns for all hydrated samples of 1:1 potassium hydrogen dioleate at 5 °C were identical with powder diffraction patterns for the corresponding anhydrous 1:1 acid–soap crystals at 5 °C. Visual inspection of hydrated samples at this temperature showed crystals suspended in a clear liquid. Wide-angle diffraction patterns of hydrated samples at 5 °C showed reflections centered at 4.5, 4.3, and 3.6 Å; these reflections are also seen in wide-angle diffraction patterns for the corresponding anhydrous 1:1 acid–soap crystals at 5 °C.

Selected X-ray data for saturated hydrated 1:1 acid–soaps are presented in Table I. The formation and swelling of the lamellar phases were analogous to those for 1:1 potassium hydrogen dioleate.

Direct and Polarized Light Microscopy. Figure 5 shows selected micrographs of hydrated 1:1 potassium hydrogen dioleate samples. After several drops of water were added to 1:1 potassium hydrogen dioleate crystals under a coverslip at 20 °C, myelin figures were observed (Figure 5A,B). For fully equilibrated hydrated samples, polarized light microscopy showed angular, striated, and nongeometrical textures (Figure 5C,E), corresponding to the hexagonal phase, and oily streak and mosaic textures (Figure 5D,E), corresponding to the lamellar phase (Rosevear, 1954, 1968; Small et al., 1966), depending on the water content. Samples at all concentrations were heated from 23 to 70 °C at a rate of 1 °C/min; no changes in optical textures were noted on heating from a temperature just above the highest transition detected by DSC to 70 °C. At 5 °C (below the lipid chain-melting transition), samples appeared as birefringent crystals in an isotropic liquid (Figure 5F). At water contents above 90% and temperatures above 11 °C, samples were turbid but no birefringence or optical textures could be visualized by polarized light microscopy.

Discussion

Phase Diagram and Phase Rule Analysis. The types of crystalline and liquid-crystalline phases formed by 1:1 potassium acid–soaps in water have been characterized by DSC,

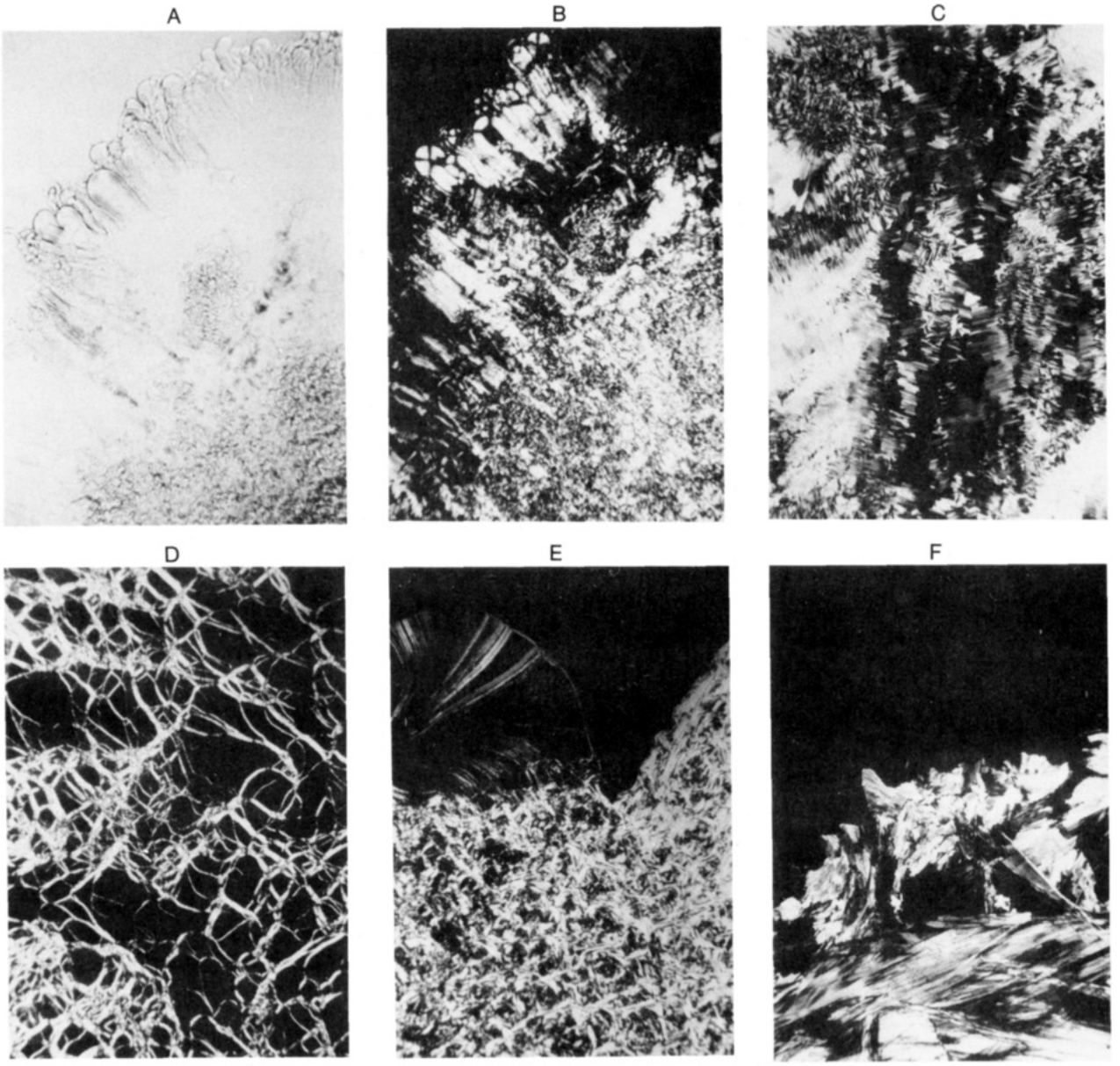

FIGURE 5: Selected direct and polarized light micrographs of hydrated 1:1 potassium hydrogen dioleate. (A and B) Crystals of acid–soap were placed between a glass slide and coverslip, and several drops of water were added to the edge of the coverslip: (A) sample after 5-min equilibration under direct light, showing myelin figures, 2.8×, 20 °C; (B) same sample under polarized light. (C) 1:1 acid–soap in 20% H_2O, fully equilibrated sample, 39 °C, 2.8×, crossed polars. Angular and striated textures characteristic of hexagonal phase (Rosevear, 1954, 1968; Small et al., 1966) are seen. (D) 1:1 acid–soap in 60% water, fully equilibrated sample, 40 °C, 2.8×, crossed polars. Oily streak texture, characteristic of lamellar phase, is seen. (E) 1:1 acid–soap in 50% water, 22 °C, 2.8×, crossed polars. Two phases are seen: (bottom) a phase exhibiting angular and striated textures and (top left) a phase exhibiting oily streak textures. (F) 1:1 acid–soap in 30% water, fully equilibrated sample, 5 °C, 2.8×, crossed polars. Birefringent acid–soap crystals are seen.

X-ray diffraction, and direct/polarized light microscopy. The results for 1:1 potassium hydrogen dioleate are summarized in the form of a temperature–composition phase rule diagram (Figure 6). Application of the Gibbs phase rule provided a theoretical framework for interpolation of the data to other temperature/composition values, prediction of the number of phases or components present in the system, and definition of the number of independent variables that need to be fixed in order to completely describe the physical state of the system.

In Figure 6, two one-phase liquid-crystalline regions are seen. First, at low water content, a hexagonal type II (inverted hexagonal) phase containing hexagonally packed cylinders of water in a matrix of lipid with lipid polar groups surrounding the water cylinders is seen. The evidence that this is hexagonal type II rather than type I (Luzzati, 1968; see Figure 7) includes the following: (i) the calculated surface areas per polar group increased with increasing water concentration; this occurs only for type II; (ii) the hexagonal phase in our samples occurred at lower water concentration with respect to the lamellar phase; the opposite occurs when the structure is type I; (iii) the hexagonal phase in our samples occurred at such low water concentrations that not enough water would be available to fill the gaps between the lipid rods if the structure were type I.

The second one-phase region, occurring at higher water concentrations, contains the lamellar liquid-crystalline phase. This consists of an ordered array of lipid bilayers with intercalated water layers. Evidence that these are noninterdigitated bilayers comes mainly from the lipid layer thickness in the presence of water (d_L), which was experimentally determined from the linear plot of first-order lamellar long spacings at 20 °C as a function of $(1 - c)/c$ (Figure 4). Extrapolation to $(1 - c)/c = 0$ yielded a value of 46 Å for d_L. The linearity of the plot suggests that the lipid bilayer structure

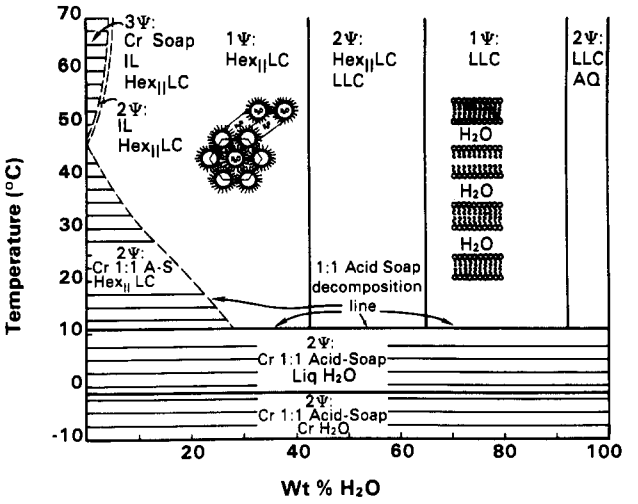

FIGURE 6: Equilibrium phase diagram of 1:1 potassium hydrogen dioleate in water. Abbreviations: Cr, crystalline, IL, isotropic liquid, AQ, aqueous phase; A–S, acid–soap; other abbreviations as in Figure 3. Dashed lines denote that the exact positions of these boundaries have not been defined in this study. The boldface horizontal lines indicate phase boundaries, and the other horizontal lines denote tie lines in invariant regions.

did not change significantly with increasing water content. For a lipid bilayer with noninterdigitated, fully extended hydrocarbon chains aligned perpendicular to the plane of the bilayer (i.e., with the cis kinks removed so that the chain is roughly linear), the estimated hydrocarbon thickness is approximately 45.7 Å, assuming each carbon extend 1.27 Å along the hydrocarbon chain axis (Piper, 1929). If the chains were interdigitated, the hydrocarbon thickness would be roughly half, or about 22.9 Å. The polar region adds another 6 Å to the bilayer (Small, 1986), making the total extended bilayer thickness about 51.7 Å for a true bilayer and 28.9 Å for an interdigitated bilayer. Since the experimentally determined and calculated d_L value (46 Å) is much greater than the maximum thickness for an interdigitated bilayer, we conclude that the lamellar liquid-crystalline phase is a true bilayered structure. The fact that the thickness (46 Å) is less than that of an extended chain bilayer is most likely because the carbon–carbon distances in a lamellar liquid crystal are somewhat less than the 1.27-Å distance per carbon found in crystalline chains (Luzzati, 1968). In fact, if the polar group thickness is subtracted from the total bilayer thickness of 45 Å and the resulting 40-Å thickness for the hydrocarbon layer or divided by 36, about 1.1 Å per carbon is obtained. This value is consistent with that found for many other liquid-crystalline systems in which the hydrocarbon chains are melted (Luzzati, 1968; Small, 1986).

The phase diagram also contains six two-phase regions: (i) between the one-phase hexagonal and lamellar regions, a region containing both of these phases; (ii) between −1 and 11 °C, at all water contents, a region consisting of crystalline 1:1 acid–soap and liquid water; (iii) below −1 °C, a region containing crystalline acid–soap and crystalline water; (iv) above 11 °C and at <30% water, a region containing 1:1 acid–soap crystals and hexagonal type II liquid crystals; (v) above 47 °C and at <10% water, and to the right of the three-phase region, a region containing isotropic liquid and hexagonal type II liquid crystals; (vi) a region at >90% H_2O and >11 °C. The exact boundaries of (iv) and (v) have not been defined in this study.

The sixth two-phase region occurs at very high water content and probably contains unilamellar vesicles in an aqueous phase. The evidence for the presence of unilamellar vesicles includes the following. First, X-ray diffraction patterns above 90% water show only a broad scattering fringe similar to that seen for vesicles or micelles (Atkinson et al., 1974). Since our samples were turbid and micellar solutions are optically clear, the broad scattering fringe probably indicates vesicular rather than micellar aggregates. Second, freeze–fracture electron microscopy results for analogous systems have demonstrated the presence of vesicles at high water concentrations (Hicks & Gebicki, 1977; Hargreaves & Deamer, 1978).

Interpretation of the phase diagram (Figure 6) in light of the Gibbs phase rule, $F = C - P + 2$,[2] gave additional information regarding the number of components present and the decomposition of the 1:1 compound. For example, in the two-phase region containing both hexagonal and lamellar liquid-crystalline phases, our X-ray data at 20 °C (Figures 2 and 3) contained two sets of long spacings corresponding to two separate phases; the long spacings for the lamellar phase increased with increasing water content over this region. Thus, P must have been ≥ 2, and $F \geq 1$. At constant temperature and pressure, $F = C - P$; therefore, C must have been >2. However, intuitively, it appeared that the system contained only two components: 1:1 acid–soap and water. There are three possible explanations for this apparent discrepancy: (i) the system was not at equilibrium, and thus, the phase rule did not apply; (ii) the system contained a contaminant third component (i.e., excess oleic acid or potassium oleate); or (iii) the 1:1 compound decomposed into its parent oleic acid and potassium oleate upon hydration and/or heating, in which case an extra component would be generated upon decomposition. The first possibility is highly unlikely because repeated measurements on the same samples over long periods of time (up to 1 year) and on different sample preparations with different thermal histories yielded identical results. Thus, the samples appeared to be at true equilibrium. The second possibility is unlikely since the stoichiometry by titration was 1:1 and neither DSC or X-ray analyses detected any oleic acid or potassium oleate in our crystalline 1:1 acid–soap samples. Therefore, the most likely explanation is the third, i.e., that, above 11 °C and 30% water, the 1:1 acid–soap compound decomposed into two compounds (oleic acid and potassium oleate) so that the resulting system contained three components: oleic acid, potassium oleate, and water. This explanation is consistent with independent observations that *liquid-crystalline* fatty acid/soap (in contrast with crystalline 1:1 acid–soap) does not require an exact 1:1 stoichiometry of fatty acid to soap (Cistola, 1985). Thus, hydrated *crystals* of 1:1 acid–soap are composed of two compounds (1:1 acid–soap and water), but hydrated *liquid crystals* of 1:1 fatty acid/soap are a mixture of three compounds: fatty acid, soap, and water.[3] The decomposition of the 1:1 compound into a mixture of fatty acid and soap compounds occurs at 11 °C at water concentrations >30% and at higher temperatures for samples containing <30% water. The decomposition line of the 1:1 compound into fatty acid and soap is marked in Figure 6. Note that the transition at 11 °C is also a chain-melting transition.

Below the decomposition temperature line, the system contains two components and two phases. Thus, the two-phase region containing crystalline acid–soap and liquid water is invariant ($F = 0$) at a fixed temperature; horizontal tie lines are drawn across this region to denote this invariance. This is true for all two-phase regions below the decomposition line. *Above* the decomposition line, the system contains three

[3] We use the following terminology to distinguish single compounds from mixtures of two compounds. "Acid–soap" indicates one compound whereas "fatty acid/soap" indicates a mixture of two compounds.

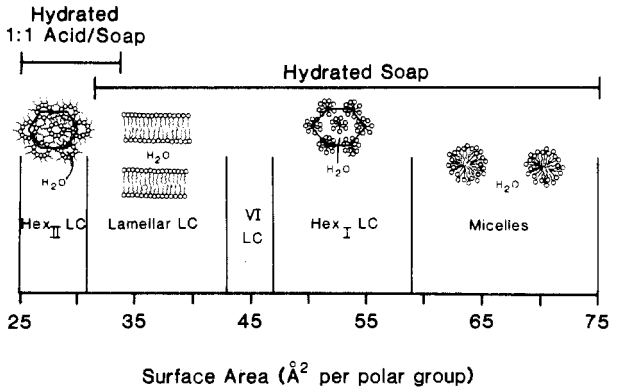

FIGURE 7: Liquid-crystalline and micellar phases and corresponding surface areas for hydrated 1:1 fatty acid/potasium soap and hydrated potassium soap systems. Abbreviations: VI, viscous isotropic; LC, liquid crystals; Hex_I, hexagonal type I; Hex_{II}, hexagonal type II. Surface area data for hydrated soaps are from Luzzati (1968) and Hauser et al. (1960); surface area data for hydrated 1:1 acid–soaps are from this study (Figure 4).

components, and therefore, at a fixed temperature, only one region is invariant (the three-phase region).

Acid–Soap Systems Containing Different Chain Types. The phase behavior, as determined by DSC, X-ray diffraction, and microscopy, of hydrated 1:1 acid–soaps with saturated hydrocarbon chains ranging from 10 to 18 carbons was qualitatively similar to oleate, except that the phase transitions were much higher (Table I). Thus, saturated as well as unsaturated fatty acid/soap/water systems can form ordered lamellar phases (Table I; Cistola, 1985) and liposomes (Hargreaves & Deamer, 1978), as long as the temperature is above the hydrocarbon chain-melting transition temperature. These findings are in contrast to the previous assertion that the presence of unsaturated fatty acids is obligatory for bilayer formation (Gebicki & Hicks, 1973, 1976).

Contrast of Hydrated Soap and Hydrated 1:1 Fatty Acid/Soap Systems. Figure 7 identifies the types of phases formed by hydrated soap/water and hydrated 1:1 fatty acid/soap systems and the surface areas per polar group of the different phases. Fully ionized potassium oleate (or any potassium or sodium soap above its chain-melting transition) forms, with increasing water concentration, lamellar, viscous isotropic, hexagonal type I, and micellar phases. The surface areas range from roughly 32 to 75 Å^2 (Husson et al., 1960; Reiss-Husson & Luzzati, 1964; Gallot & Skoulios, 1966). Hydrated 1:1 oleic acid/potassium oleate, as shown in this study, forms hexagonal type II and lamellar (bilayer) phases, with surface areas ranging from 26 to 33 Å^2 per polar group.

Hydrated 1:1 fatty acid/soap mesophases exhibit smaller surface areas and a smaller range of surface areas than the mesophases of hydrated soaps (Figure 7). Since the counterions and hydrocarbon chain types are matched in these two systems, the only remaining variable is the number of charges per polar group (or surface charge density). The soaps have one negative charge per polar group, whereas the 1:1 fatty acid/soaps have one negative charge per every *two* polar groups. Thus, the hydrated soap experiences a greater lateral charge repulsion between polar groups in the plane of the bilayer, giving rise to greater surface areas per polar group and to liquid-crystalline or micellar phases that can accommodate those greater surface areas. Since the 1:1 fatty acid/soap mixture experiences less charge repulsion, surface areas are smaller, and liquid-crystalline phases that are formed can accommodate those smaller surface areas. Thus, the number of charges per polar group (or the ionization state) determines the *type* of structures formed by "fatty acids" in water.

Another significant difference between hydrated potassium soaps and hydrated potassium 1:1 acid–soaps is the lack of formation of a gel phase by the latter. Potassium soaps in water form a gel phase (with interdigitated lipid bilayers) below their chain-melting temperature (Vincent & Skoulios, 1964; Vincent, 1964). The surface areas per polar group for this phase (39–40 Å^2) would result in substantial charge repulsion if the polar groups were aligned in the same plane, but they are staggered in and out of the plane of the bilayer surface, effectively reducing charge repulsion without changing the surface area per polar group in the plane of the bilayer. In this study, we have shown that hydrated potassium acid–soaps do not form metastable or stable gel phases. Since the lipid enthalpies extrapolate to zero at 100% water (Figure 1C), it can be inferred that little or no bound water was associated with lipid below the chain-melting transition. In contrast, a gel phase would contain substantial bound water. In addition, small- and wide-angle X-ray diffraction data, collected at 1 °C temperature intervals in the vicinity of the crystalline to liquid-crystalline phase transition, have not detected any gel phases for the acid–soap system. The lack of formation of a gel phase by hydrated acid–soaps may be explained by the reduced number of negatively charged polar groups in this system as compared with hydrated potassium soaps. There is a lower degree of charge repulsion in the former and, therefore, less tendency to form an interdigitated gel phase with staggered polar groups.

Comparison of 1:1 Fatty Acid/Soap/Water with Other Lipid/Water Systems. The type and progression (with increasing hydration) of liquid-crystalline phases formed by hydrated 1:1 fatty acid/potassium soap mixtures are not unique to these systems. The following systems also exhibit hexagonal type II and lamellar liquid-crystalline phases with increasing hydration: (1) fatty alcohol/soap/water (Dervichian & Magnant, 1946; Ekwall et al., 1969), (2) phosphatidylserine/water (Hauser et al., 1982), (3) human brain lipids/water (Luzzati & Husson, 1962), and (4) mitochondrial lipids/water (Gulik-Kryzwicki et al., 1967). Also, cholesterol/soap/water (White, 1907–1908), cholesterol ester/soap/water (Dervichian, 1946; Dervichian & Magnant, 1946), "fatty acid"/lysolecithin/water (Jain et al., 1980), and phosphatidic acid/water (Hauser & Gains, 1982) form myelin figures and swollen lamellar phases at high water content. All of the above systems have roughly one negative charge for every two hydrocarbon moieties. Thus, this particular balance of polar group charge repulsion and hydrophobic chain interactions seems to stabilize these structures. The general conditions that stabilize mesophase structures in many lipid/water systems have been discussed in more detail elsewhere (Dervichian, 1946; Parsegian, 1966; Small, 1968, 1986; Gulik-Kryzwicki et al., 1969; Ekwall, 1975; Tanford, 1980; Hauser, 1984). Specifically, for "fatty acid"/water systems, the balance of forces imposed by the presence of roughly equimolar charged (soap) and uncharged (fatty acid) polar groups explains why "fatty acids" near half-ionization (above their chain-melting transition) form bilayers rather than micelles at high water concentration and inverted hexagonal rather than lamellar phases at low water concentration.

There has been some disagreement in the literature regarding the relative importance of forces that stabilize fatty acid/soap aggregates in water. Some workers have suggested that these aggregates are a series of dimers stabilized by very strong hydrogen bonds between carboxyl and carboxylate

groups of the fatty acid and soap, respectively (Smith & Tanford, 1973; Gebicki & Hicks, 1976). These bonds probably exist in the anhydrous crystalline state for 1:1 acid–soaps (Speakman & Mills, 1961). However, the hydrated liquid-crystalline state does not require the formation of strongly hydrogen bonded dimers to stabilize bilayer and hexagonal structures. This can be deduced from several lines of evidence. First, a variety of lipid/water systems can form bilayer and hexagonal structures (see above); few of these systems have carboxyl or carboxylate groups capable of participating in such strong, specific hydrogen bonds. Second, bilayer aggregates of fatty acid/soap remain stable at fatty acid/soap ratios that deviate significantly from 1:1 (Cistola, 1985). For example, for 0.08 M oleic acid/potassium oleate at 40 °C, the lamellar phase is stable up to a fatty acid/soap ratio of 1:3 (Cistola, 1985). At this ratio, only half of the lipid molecules could participate in specific carboxyl–carboxylate hydrogen bonds. Third, at the surface of a bilayer, carboxyl(ate)–water hydrogen bonds could compete with, and would seemingly be more favorable than, carboxyl–carboxylate hydrogen bonds because of the angular restrictions of the latter. Fourth, hydrated fatty acid/soap lamellar phases at half-ionization become unstable when the hydrocarbon chain length is less than 8–10 carbons (Cistola and Small, unpublished observations), suggesting that hydrocarbon chain interactions are necessary to stabilize these phases. Therefore, it is probably more correct to view fatty acid/soap aggregates as *extended structures* stabilized primarily by a balance of polar group charge repulsion and hydrocarbon chain interactions rather than *dimers* held together primarily by strong carboxyl–carboxylate hydrogen bonds.

Biological Applications. Knowledge of the physical states of fatty acids in water aids in understanding the physical states formed by free fatty acids during their transport and metabolism in the intestine, in the circulation, and in cells. For example, in the circulation, large quantities of free fatty acids are liberated by the action of lipoprotein lipase on triglyceride-rich lipoproteins such as chylomicrons. Under certain conditions, such as low albumin concentrations, chylomicrons have been shown (by electron microscopy) to form bilayers lamellar surface extensions during lipase digestion in vitro (Blanchette-Mackie & Scow, 1976). Similar lamellar structures have been shown in adipose tissue (Blanchette-Mackie & Scow, 1981) and heart tissue (Wetzel & Scow, 1984) under conditions that cause lipolysis and accumulation of fatty acids. In all cases, these lamellar structures were believed to result from the formation of bilayers by free fatty acids liberated during lipolysis. Our studies show that free fatty acids could form bilayer structures during lipolysis in vivo if the fatty acids are near half-ionization, which would be the case if the pH is near 7.4.

ACKNOWLEDGMENTS

We thank David Jackson for software development, routine maintenance of the X-ray diffraction equipment, and expert technical assistance during X-ray data collection. We also thank Irene Miller for her expert clerical assistance in preparing the manuscript.

Registry No. $Me(CH_2)_8CO_2H$, 334-48-5; $Me(CH_2)_{10}CO_2H$, 143-07-7; $Me(CH_2)_{12}CO_2H$, 544-63-8; $Me(CH_2)_{14}CO_2H$, 57-10-3; $Me(CH_2)_{16}CO_2H$, 57-11-4; (*Z*)-$Me(CH_2)_7CH{=}CH(CH_2)_7CO_2H$, 112-80-1; potassium hydrogen dioleate, 22882-82-2; potassium hydrogen didecanoate, 21907-75-5; potassium hydrogen dilaurate, 14933-00-7; potassium hydrogen dimyristate, 3354-60-7; potassium hydrogen dipalmitate, 3354-61-8; potassium hydrogen distearate, 3354-62-9.

REFERENCES

Atkinson, D., Hauser, H., Shipley, G. G., & Stubbs, J. M. (1974) *Biochim. Biophys. Acta 339*, 10–29.
Barratt, M. D., & Laggner, P. (1974) *Biochim. Biophys. Acta 363*, 127–133.
Blanchette-Mackie, E. J., & Scow, R. O. (1976) *J. Lipid Res. 17*, 57–67.
Blanchette-Mackie, E. J., & Scow, R. O. (1981) *J. Ultrastruct. Res. 77*, 295–318.
Chevreul, M. E. (1823) *Recherches Chimiques sur les Corps gras d'Origine Animale*, pp 34, 53, and 408, Paris.
Cistola, D. P. (1985) Ph.D. Dissertation, Boston University, Boston.
Cistola, D. P., Small, D. M., Atkinson, D., & Hamilton, J. A. (1983) *JAOCS, J. Am. Oil Chem. Soc. 60*, 731.
Cistola, D. P., Small, D. M., Atkinson, D., & Hamilton, J. A. (1985) *Biophys. J. 47*, 45a.
Dervichian, D. G. (1946) *Trans. Faraday Soc. 42B*, 180–187.
Dervichian, D. G., & Magnant, C. (1946) *Bull. Soc. Chim. Biol. 28*, 419–426.
Ekwall, P. (1937) *Kolloid-Z. 80*, 77–100.
Ekwall, P. (1975) *Adv. Liq. Cryst. 1*, 1–142.
Ekwall, P., Mandell, L., & Fontell, K. (1969) *J. Colloid Interface Sci. 31*, 508–529.
Gallot, B., & Skoulios, A. E. (1966) *Kolloid-Z. Z. Polym. 208*, 37.
Gebicki, J. M., & Hicks, M. (1973) *Nature (London) 243*, 242–244.
Gebicki, J. M., & Hicks, M. (1976) *Chem. Phys. Lipids 16*, 142–160.
Goddard, E. D., Goldwasser, S., Golikeri, G., & Kung, H. C. (1968) *Adv. Chem. Ser. 84*, 67–77.
Gulik-Krzywicki, T., Rivas, E., & Luzzati, V. (1967) *J. Mol. Biol. 27*, 303–322.
Gulik-Krzywicki, T., Tardieu, A., & Luzzati, V. (1969) *Mol. Cryst. Liq. Cryst. 8*, 285–291.
Hamilton, J. A., & Cistola, D. P. (1986) *Proc. Natl. Acad. Sci. U.S.A. 83*, 82–86.
Hargreaves, W. R., & Deamer, D. W. (1978) *Biochemistry 17*, 3759–3768.
Hauser, H. (1984) *Biochim. Biophys. Acta 772*, 37–50.
Hauser, H., & Gains, N. (1982) *Proc. Natl. Acad. Sci. U.S.A. 79*, 1683–1687.
Hauser, H., Paltauf, F., & Shipley, G. G. (1982) *Biochemistry 21*, 1061–1067.
Hicks, M., & Gebicki, J. M. (1977) *Chem. Phys. Lipids 20*, 243–252.
Husson, F., Mustacchi, H., & Luzzati, V. (1960) *Acta Crystallogr. 13*, 668–677.
Jain, M. K., van Echfeld, C. J. A., Ramirez, F., de Gier, J., de Haas, G. H., & van Deenen, L. L. M. (1980) *Nature (London) 284*, 486–487.
Kantor, H. L., & Prestegard, J. H. (1978) *Biochemistry 17*, 3592–3597.
Luzzati, V. (1968) in *Biological Membranes* (Chapman, D., Ed.) pp 71–123, Academic Press, London.
Luzzati, V., & Husson, F. (1962) *J. Cell Biol. 12*, 207–219.
McBain, J. W., & Stewart, A. (1927) *J. Chem. Soc.*, 1392–1395.
McBain, J. W., & Field, M. C. (1933a) *J. Phys. Chem. 37*, 675–684.
McBain, J. W., & Field, M. C. (1933b) *J. Chem. Soc.*, 920–924.
McBain, J. W., & Stewart, A. (1933) *J. Chem. Soc.*, 924–928.
Müller, A. (1932) *Proc. R. Soc. London, A 138*, 514.

Parsegian, V. A. (1966) *Trans. Faraday Soc. 63*, 848.
Piper, S. H. (1929) *J. Chem. Soc.*, 234-239.
Ptak, M., Egret-Charlier, M., Sonson, A., & Bouloussa, O. (1980) *Biochim. Biophys. Acta 600*, 387-397.
Reiss-Husson, F., & Luzzati, V. (1964) *J. Phys. Chem. 68*, 3504.
Rosevear, F. B. (1954) *J. Am. Oil Chem. Soc. 31*, 628-639.
Rosevear, F. B. (1968) *J. Soc. Cosmet. Chem. 19*, 581-594.
Small, D. M. (1968) *J. Am. Oil Chem. Soc. 45*, 108-119.
Small, D. M. (1986) *Handb. Lipid Res. 4*, 1-672.
Small, D. M., Bourges, M., & Dervichian, D. G. (1966) *Biochim. Biophys. Acta 125*, 563-580.
Smith, R., & Tanford, C. (1973) *Proc. Natl. Acad. Sci. U.S.A. 70*, 289-293.
Speakman, J. C., & Mills, H. H. (1961) *J. Chem. Soc.*, 1164-1175.
Tanford, C. (1980) *The Hydrophobic Effect*, Interscience, New York.
Taylor, M. A., & Princen, L. H. (1979) in *Fatty Acids* (Pryde, E. H., Ed.) pp 195-217, American Oil Chemists' Society, Champaign, IL.
Vincent, J. M. (1964) Thesis, A la Faculte des Sciences de L'Universite de Strasbourg.
Vincent, J. M., & Skoulios, A. (1964) *C. R. Hebd. Seances Acad. Sci. 258*, 1229.
Wetzel, M. G., & Scow, R. O. (1984) *Am. J. Physiol. 246*, C467-C485.
White, C. P. (1907-1908) *Med. Chron. 47*, 403-421.

Interaction of Short-Chain Lecithin with Long-Chain Phospholipids: Characterization of Vesicles That Form Spontaneously†

N. Elise Gabriel and Mary F. Roberts*
Department of Chemistry, Massachusetts Institute of Technology, Cambridge, Massachusetts 02139
Received October 23, 1985; Revised Manuscript Received January 30, 1986

ABSTRACT: Stable unilamellar vesicles formed spontaneously upon mixing aqueous suspensions of long-chain phospholipid (synthetic, saturated, and naturally occurring phosphatidylcholine, phosphatidylethanolamine, and sphingomyelin) with small amounts of short-chain lecithin (fatty acid chain lengths of 6-8 carbons) have been characterized by using NMR spectroscopy, negative staining electron microscopy, differential scanning calorimetry, and Fourier transform infrared (FTIR) spectroscopy. This method of vesicle preparation can produce bilayer vesicles spanning the size range 100 to greater than 1000 Å. The combination of short-chain lecithin and long-chain lecithin in its gel state at room temperature produces relatively small unilamellar vesicles, while using long-chain lecithin in its liquid-crystalline state produces large unilamellar vesicles. The length of the short-chain lecithin does not affect the size distribution of the vesicles as much as the ratio of short-chain to long-chain components. In general, additional short-chain decreases the average vesicle size. Incorporation of cholesterol can affect vesicle size, with the solubility limit of cholesterol in short-chain lecithin micelles governing any size change. If the amount of cholesterol is below the solubility limit of micellar short-chain lecithin, then the addition of cholesterol to the vesicle bilayer has no effect on the vesicle size; if more cholesterol is added, particle growth is observed. Vesicles formed with a saturated long-chain lecithin and short-chain species exhibit similar phase transition behavior and enthalpy values to small unilamellar vesicles of the pure long-chain lecithin prepared by sonication. As the size of the short-chain/long-chain vesicles decreases, the phase transition temperature decreases to temperatures observed for sonicated unilamellar vesicles. FTIR spectroscopy confirms that the incorporation of the short-chain lipid in the vesicle bilayer does not drastically alter the gauche bond conformation of the long-chain lipids (i.e., their transness in the gel state and the presence of multiple gauche bonds in the liquid-crystalline state).

Since the original demonstration by Bangham et al. (1965) that aqueous dispersions of phospholipids were capable of forming closed spherical structures encapsulating aqueous compounds, liposomes have been widely studied as models for cell membranes. Such bilayer vesicles have also been used for functional reconstitution of membrane-bound proteins [for example, see Christianson and Carlsen (1983)], as substrates for a variety of lipolytic enzymes (Kensil & Dennis, 1979; DeBose & Roberts, 1983), as permeability barriers in transport studies (Papahadjopoulos & Watkins, 1967; Paphadjopoulos & Kimelberg, 1973; Racker & Stoeckenius, 1974), and for encapsulation of various agents for assays, drug delivery, etc. (Ryman & Tyrrell, 1980). While multilamellar structures form readily, unilamellar vesicles are more analogous to real cell membranes. Several methods have been developed [for a review, see Gregoriadis (1984)] to form unilamellar vesicles from pure lecithin multibilayers, including (i) sonication, (ii) reverse evaporation from organic solvent, (iii) detergent dialysis, and (iv) pressure/mechanical filtration. All of these methods either require expensive equipment [sonicator, French press (Hamilton et al., 1980)] or depend on the addition and partial removal of nonphospholipid material (organic solvent, detergents) and hence are multistep processes. In some cases, the inclusion of sufficient amounts of phosphatidic acid with the lecithin matrix can be used to induce unilamellar vesicle formation by pH shifts (Hauser, 1983).

† This research was supported by NIH Grant GM 26762.

0006-2960/86/0425-2812$01.50/0 © 1986 American Chemical Society